ChemComm

Accepted Manuscript

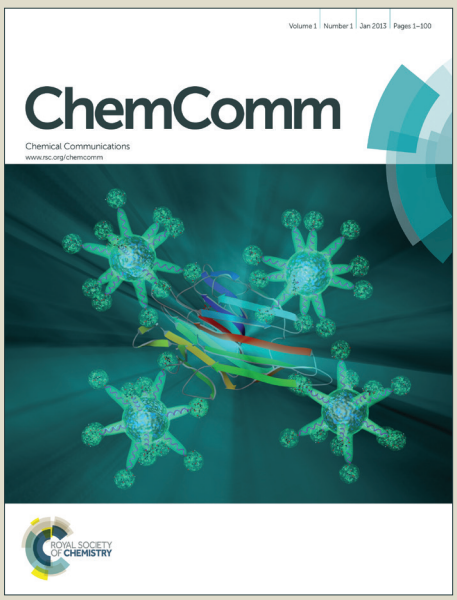

ROYAL SOCIETY OF CHEMISTRY

www.rsc.org/chemcomm

Journal Name

RSCPublishing

COMMUNICATION

Novel Nanogel-based Fluorescent Probe for Ratiometric Detection of Intracellular pH Values

Cite this: DOI: 10.1039/x0xx00000x

Lixia Cao,[a] Xiaoyan Li, [a] Wangshuang Qing,[a] Shayu Li, *[a] Yi Li*[b]and Guoqiang Yang*[a]

Received 00th January 2012,
Accepted 00th January 2012

DOI: 10.1039/x0xx00000x

www.rsc.org/

A new nanogel indicator (NGI) for ratiometric fluorescent detection of intracellular pH value has been reported. In aqueous solution, the NGI can be ratiometric sensing of pH changes with a large hypsochromic shift of 100 nm in green-red region and reversible. Furthermore, the NGI has been used to calibrate cytosol pH value in living cells.

Intracellular pH (pHi) is a crucial factor in cell metabolism processes, virtually all proteins depend on pH to maintain their structure and function.[1] In addition it serves as an important role in many biological processes such as cell proliferation,[2] apoptosis,[3] drug resistance, phagocytosis,[4] endocytosis[5] and signal transduction.[6] The proton motive force induced by pH gradients also very important in the generation and conversion of cellular energy.[7] Moreover, it was recently reported that cytosolic pH has a strong influence on phosphocreatine recovery.[8] As far as known, pHi is strictly regulated in cellular space. Slight abnormality of pHi level may result in clinical problems, such as cancer, Alzheimer's disease,[9] etc. More extreme deviation can be fatal. Thus, in-vivo monitoring of pHi changes is of great importance for precise understanding the relation between pHi level and cellular process.[10] However, the classical quantification methods cannot carry the heavy responsibility because of their low spatial resolution (microelectrodes) or complicated operations (NMR). It is necessary to develop fast and convenient approaches for the monitoring of pHi level.

Fluorescence-based detection technique using high resolution microscopy is the most powerful method in modern cell research because of its high sensitivity, nondestructive character, great choice of dyes and less influence on test cells.[11] To date, several kinds of fluorescent dyes have been reported for mapping pHi level. 2', 7'-bis-(2-carboxyethyl)-5-(and 6)-carboxyfluorescein(BCECF), 1, 4-dihydroxyphthalonitrile(DHPN), seminaphthorhoda-fluors (SNARF-1) and their derivatives are the most widely used pHi indicators. All these indicators display a desirable pH-dependent fluorescence emission during ionization and deionization processes.[12] However, BCECF family only show obvious optical changes in terms of fluorescence intensity rather than profile, which can be significantly influenced by the excitation power and have to be taken more accurate calibration.[13] DHPN is a ratiometric fluorescence probe that can efficiently self-calibrate to exclude the environment effects, but the small difference (30 nm) in wavelength between the two emission bands limits its effectiveness.[14] SNARF-1 shows more desirable wavelength gap (60 nm) characteristics and has been used in flow cytometry and microscopy measurements. The main drawbacks are its low fluorescence efficiency (max 0.09) and fast photobleaching rate.[15] Thus, it is a great challenge to design new ratiometic pHi indicators with high quantum yield, significant color change and photostability. Moreover, besides performance improvements, the cost is also a factor that has to be considered in practical application.

Herein we describe a composite dual-emissive pHi indicator that allows in-vivo detection of pHi 4-10 in cytosol. This easy-fabricated indicator shows excellent photostability comparable to above well-known dyes. In design of the indicator, we chose pyrene as fluorophore and functionalized it with a hydroxyl group and an aldehyde group to synthesize 8-hydroxypyrene-1-carbaldehyde (HPC). Similar to fluorescein family and DHPN, HPC also operates through protonation and deprotonation of phenolic hydroxyl moiety (Fig. 1a). The simple and large conjugate structure restricts the nonradiative pathway and promises the potential high luminescent quantum yield of HPC molecule either in phenol form or in anionic form. Electron-withdrawing aldehyde group amplifies the difference in electron-donating ability of hydroxyl group and anionic oxygen, which makes the wavelength difference of dual emission bands reach up to 100 nm, an amazing value that very facilitates the ratiometric emission detection.

Water-solubility and interaction with biomolecules are always the major problems for the organic dyes used as intracellular probes, and HPC is no exception. The solubility of HPC does not exceed 0.1 μM even in pH 12 water. Meanwhile, its two active groups may interact with biomolecules or organelles, resulting in the possible changes of luminescent properties. To address these issues, we chose polyurethane nanogel as carrier of HPC molecules to prepare the composited indicator taking into account the uncertainty of chemical modification. The polyurethane hydrogel is known for its stability, biocompatibility and, most importantly, nonresponsive to pH variation of the media.[16] The details of HPC synthesis, nanogel preparation and indicator fabrication are provided in the supporting information.

a)

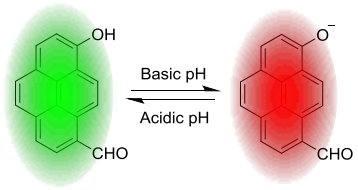

b)

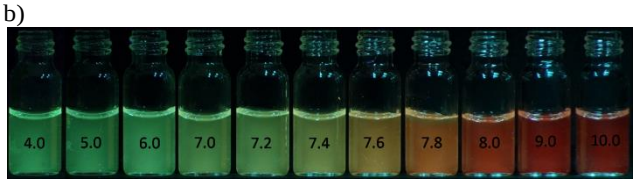

Fig. 1 a) Mechanism of emission changes with pH value. b) Photography of fluorescence of NGIs at different pH value.

The appearance and size distribution of the nanogel indicator (NGI) were detected with field emission scan electron microscopy (SEM) and dynamic light scattering (DLS). The SEM sample was prepared by freeze-drying method to keep native appearance of the particles in wet state. The NGIs are irregular spheres with multi-dispersion (Fig. S1a) and no fine surface structure is observed even under 150000 times magnification, indicating that the size of pore in the network is not greater than 1.5 nm. In DLS measurements, the NGIs show a monomodal size distribution with a hydrodynamic diameter of 92 nm (Fig. S1b). This particle size distribution suggests that the NGI is more suitable for cytosol pHi purpose than organelle pHi detection.

The NGI displays a pH-dependent fluorescence change from bright green to red with relatively high quantum yields over a wide pH range of 4.0-10.0 (Table 1). This intense fluorescence emission produces a high signal/noise ratio that is appreciate for reliable pHi measurement. The continuous pH-dependent change in fluorescence color can be observed on a conventional UV illuminator (Fig. 1b). The Commission Internationale de L'Eclairage (CIE) 1931 (x,y) chromaticity diagram of NGI fluorescence in different pH solutions are shown in Fig. S2. It is easy to determine the pH value according to the diagram with the fluorescence, making it appropriate for preliminary and wide-scope observation of pHi distribution.

Table 1 Quantum yields Φ of NGIs in water at various pH values.

pH	4.0	5.0	6.0	7.0	7.2	7.4	7.6	7.8	8.0	9.0	10.0
Φ	0.24	0.23	0.22	0.21	0.20	0.19	0.18	0.17	0.16	0.15	0.14

The NGI is made up of 0.5% HPC and 99.5% nanogel (weight ratio). Its absorption and fluorescence spectroscopy in sodium phosphate buffer solutions with different pH values are shown in Fig 2. The luminescence of NGIs is based on the HPC population of phenol and anionic forms. Under acid pH conditions, NGIs show a sharp absorption band at 430 nm and a bimodal luminescence, consisting of a major band around 510 nm (phenol form) and a minor fraction around 610 nm (anionic form). The increase of pH value strongly influences the dynamic equilibrium between the two emissive forms and results in gradual changes in the absorption and emission spectra. An isosbestic point and an isoemissive point, respectively, can be observed at 453 nm and 570 nm. So the ratio of fluorescence intensities from the two different molecular forms (I_{510}/I_{610}) can be measured and related to the pH level (Fig. 2b). Almost a linear relationship of the intensity ratio with pH velue is observed in the physiological range (pH 6−8), making NGIs promising as a candidate of good indicator for pHi sensing. The pKa value of NGIs is 7.8±0.1, calculated using the Henderson-Hasselbach-type mass action equation log(Imax-I)/(I-Imin)=pH-pKa,[17]where Imax, Imin, and I represent the maximum, minimum, and observed fluorescence intensity at a given pH value, respectively. The value is very close to the physiological pH 7.4, further indicating the NGIs is an innate pHi indicator in bio-system.

a) b)

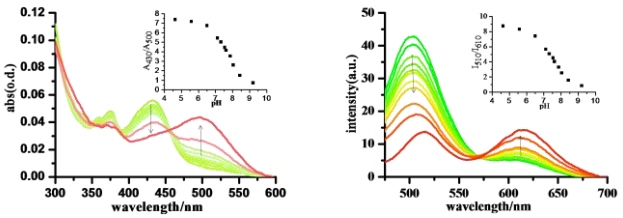

Fig. 2 a) UV/Vis absorption spectra of NGIs (HPC, 1.0 μm) at various pH values (arrows show direction of pH increase from 4.0 to 10.0). b) Fluorescence emission spectra of NGIs at various pH values (excitation: 455 nm). Inset a): The function of absorption ratio (A_{430}/A_{500}) versus pH value. Inset b): Plot of fluorescence intensity ratio (I_{510}/I_{610}) versus pH. All data were obtained in phosphate buffer solution at 37 °C.

The intracellular environment is complicated, with thousands of different biomolecules alongside many other types of molecules and ions. To determine whether biological molecules might affect the pH measurement, we measured the fluorescence spectra of NGIs in the presence of essential ions, glycine, human serum albumin (HSA) and H_2O_2 under physiological conditions (PBS buffer, pH=7.4, 37 ℃). Glycine, HSA and H_2O_2, respectively, were chosen as representatives of numerous small biomolecules, biomacromolecules and reactive oxygen species (ROS). As can be seen from Fig. 3a, almost no spectroscopic changes are observed when NGIs are exposed to those anions, cations, amino acid, protein and ROS. This excellent tolerance for the environmental substances is in keeping with expectations. HPC is designed to have no coordination effect to any ions and HSA is too large to be adsorbed into the nanogel network. Glycine is the smallest of the 20 amino acids commonly found in proteins and is possible to be entrapped into nanogel, but it is also hard to react with HPC as demonstrated in the experiment. For the case of H_2O_2, it almost has no influence on the NGIs, similar to that of Glycine. Meanwhile, considering that thiol group could react with the aldehyde easily, we tested whether cysteine can affect the NGIs. The result shows that cysteine has almost no effect on NGIs. In addition, the NGIs exhibit an easily reversible fluorescence emission around pH 4-10 (Fig. S3). These results illustrate that the NGIs can instantly respond to the change of pH value without interference by the surrounding environment.

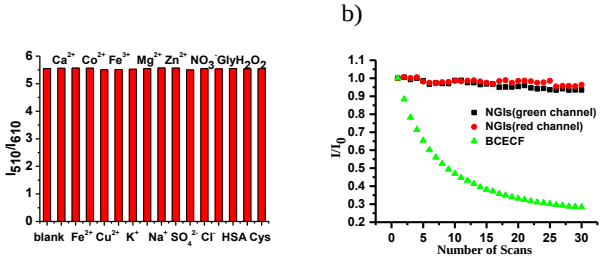

Fig. 3 a) Fluorescence responses of NGIs in PBS (pH=7.4) to diverse substances; 1, blank; 2, Ca^{2+} (10 mM); 3, Fe^{2+} (1 mM); 4, Co^{2+} (1 mM); 5, Cu^{2+} (1 mM); 6, Fe^{3+} (1 mM); 7, K^+ (10 mM); 8, Mg^{2+} (10 mM); 9, Na^+ (10 mM); 10, Zn^{2+} (1 mM); 11, SO_4^{2-} (10 mM); 12, NO_3^- (10 mM); 13, Cl^- (10 mM); 14, Gly (0.1 mM); 15, HSA (0.1 mM); 16, H_2O_2 (0.1 mM); 17, Cysteine (0.1 mM); b) Signal loss (%) of fluorescent emission of NGIs (black and red) and BCECF (green) in vivo with increasing number of scans. Excitation with 458 nm.

For an indicator to be really used in living cells, its biocompatibility is always the first and foremost important criterion to be evaluated. The cytotoxicity of the NGIs on NIH/3T3 Fibroblasts is determined by standard 3-(4, 5-dimethyl-2-thiazolyl)-2, 5-diphenyltetrazolium bromide (MTT) assay. The MTT results show that the cell viability is not obviously affected by NGIs even when HPC concentration is as high as 5.0 μM (Fig. S4). Cell membrane permeability is another important factor for evaluating the in vivo indicator. An indicator with poor permeability can only be used via microinjection, electroporation, and scrape loading to load inside living cells, which might damage the cells. As shown in Fig. S5, Fibroblasts cells incubated with NGIs (1 μM HPC) for 30 min present strong fluorescence in the green channel and weak fluorescence in the red channel, confirming the good permeability of NGI. In addition, photostability is an issue that has to be considered for the probe dyes in cell imaging because a harsh laser beam as excitation source would quickly photobleach the fluorescence of the molecules. Thence we compared the stability of NGI with commercial pHi indicator—BCECF in vivo with the same excitation conditions. The experimental results demonstrate that NGIs presents much better photostability than BCECF (Fig. 3b). Moreover, detailed fluorescence images show that NGIs is localized all over the cytosol, which is in line with expectations because of the size of NGI and its very low affinity for biomolecules. The nontoxicity, good permeability, good localization and excellent photostability demonstrate the applicability of NGIs in vivo.

All above preliminary results of the NGI urge us to further investigate its practical performance in cell images. Fig. 4 shows the effects on pHi of a 30 min exposure to buffer media with various pH levels at 37 ℃. Ionophore nigericin was employed to induce a rapid exchange of K^+ for H^+ to rapidly homogenize pHi with extracellular pH.[18] The living cells stained with the NGIs at pH 6.0 present a bright fluorescence in the green channel and almost no fluorescence in the red channel. When the pHi value increases from 6 to 9, the fluorescence intensity gradually decreased in the green channel and the fluorescence emission in the red channel shows the opposite trend. The intensity changes are confirmed by in-situ spectral measurements (Fig. S6). Since the ratio of the red-to-green signals from the two channels directly relates to the local pH value, monitoring of pHi in cytosol can be achieved through analysis of the ratio images. The area with higher pseudo color temperature, corresponding to a low red-to-green ratio, indicates an acidic environment, while the lower pseudo color temperature suggests a higher pH value. There are individual differences among the cells in the ratiometric images, but a tendency that the perinuclear regions show higher pH can be observed, which may be the result of neutralization from the mitochondria with higher local pH in living cells.[19]

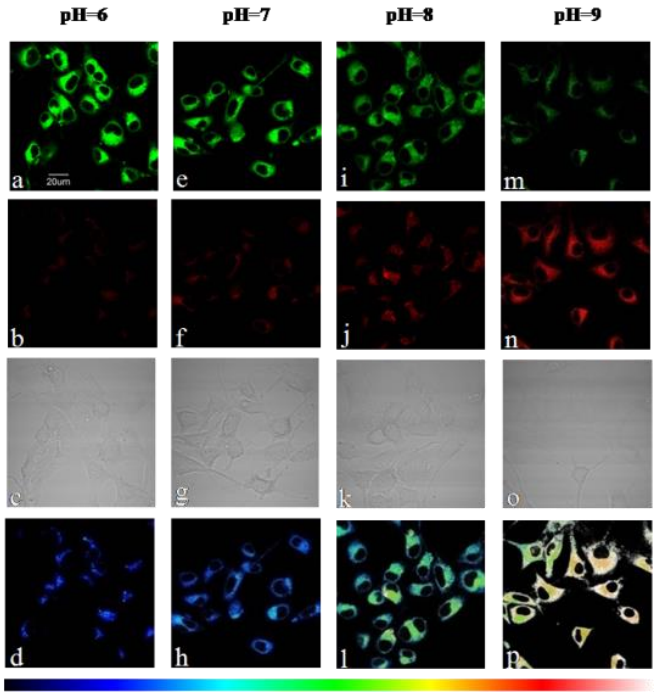

Fig. 4 Confocal microscopy images of NGIs (HPC, 1.0 μM) in NIH/3T3 Fibroblasts cells clamped at pH 6 (a–d), 7 (e–h), 8(i–l) and 9(m-p) The excitation wavelength was 458 nm and the images were collected at 470–510 nm (first row,) and 570–630 nm (second row). The corresponding contrast images (third row) and ratio images obtained from the green and red channels (fourth row). The bottom color strip represents the pseudocolor change with pH. Scale bar, 20 μm.

Encouraged by the results of above artificial pHi adjustment, we were interested in applying the NGI to monitoring the real process involving pHi changes. Redox is the central chemical reaction at cellular level and intracellular ROS has been reported to show important influences on pHi homeostasis.[20] To monitor the effects of ROS on pHi level in cytosol, NIH/3T3 Fibroblasts cells loaded with the NGIs were exposed to H_2O_2 (100 μM). We imaged the fluorescence changes of NGIs with time upon the addition of H_2O_2 (Fig. 5). Obviously, in the first 30 minutes the introduction of H_2O_2 leads to a gradual intracellular acidosis from site near the cell membrane to the place closing to the nucleus. The average ratio (Igreen/Ired) increases from 0 minute to 30 minutes, giving a corresponding change of pH value from 7.4 to 7.0. This cytosolic acidosis should originate from hydroxyl free radicals produced by H_2O_2 oxidation.[21] In addition, hydroxyl free radicals could inhibits glycolysis and induce the hydrolysis of intracellular ATP, which cause H^+ imported and redistributed from acidified organelles to cytosolic compartments.[22]

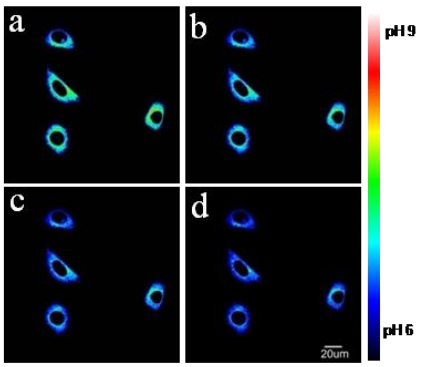

Fig. 5 Ratiometric images of NGIs-loaded NIH/3T3 Fibroblasts cells in PBS (pH=7.4): a) intact cells, and cells treated with H_2O_2 for b) 10min c) 15min d) 30min. The excitation wavelength was 458 nm .Scale bar: 20μm.

Conclusions

In this work, a ratiometric fluorescent pHi indicator NGI has been developed by incorporating a novel phenolic dye HPC into polyurethane nanogel. The NGI shows a desirable fluorescence response for pH changes with an appropriate 100 nm emission shift and adaptable pKa in the physiological range. Possessing low cytotoxicity, good permeability and dispersibility, high reversibility and excellent photostability, the NGI is a well-suited imaging indicator for pHi distribution and change tracking. Quantitative determinations of pHi of intact NIH/3T3 Fibroblasts cells have been successfully performed with the NGIs. In terms of fluorescence ratiometry, the H_2O_2 induced cytosolic acidosis has been monitored. Moreover, because of the capacity of the nanogels, NGI can be further modified as a multifunctional agent for an array of applications.

Acknowledgements

We are grateful for funding from the National Basic Research Program (2013CB834505, 2013CB834703, 2011CBA00905, and 2009CB930802) and the National Natural Science Foundation of China (Grant Nos. 21073206, 21072196, 21233011, and 21205122).

Notes and references

[a]Beijing National Laboratory for Molecular Sciences, Key Laboratory of Photochemistry, Institute of Chemistry, Chinese Academy of Sciences, Beijing 100190, China

[b]Key Laboratory of Photochemical Conversion and Optoelectronic Materials, Technical Institute of Physics and Chemistry, Chinese Academy of Sciences, Beijing 100190, China

†Electronic Supplementary Information (ESI) available: See DOI: 10.1039/c000000x/

1. S. T. Whitten, E. B. Garcia-Moreno and V. J. Hilser, *Proc. Natl. Acad. Sci.*, 2005, **102**, 4282–4287.
2. D. Perez-Sala, D. Collado-Escobar and F. J. Mollinedo, *Biol. Chem.*, 1995, **270**, 6235.
3. D. Lagadic-Gossmann, L. Huc and V. Lecureur, *Cell Death Differ.*, 2004, **11**, 953–961.
4. M. Miksa, H. Komura, R. Wu, K. G. Shah and P. J. Wang, *Immunol. Methods.*, 2009, **342**, 71.
5. M. Lakadamyali, M. J. Rust, H. P. Babcock and X. Zhuang, *Proc. Natl. Acad. Sci.*, 2003, **100**, 9280.
6. S. Yao, K. J. Schafer-Hales and K. D. Belfield, *Org. Lett.*, 2007, **9**, 5645-5648.
7. J. R. Casey, S. Grinstein and J. Orlowski, *Nat. Rev. Mol. Cell Biol.*, 2010, **11**, 50–61.
8. S. M. Pancera, H. Gliemann, T. Schimmel and D. F. S. Petri, *J. Phys. Chem.*, 2006, **110**, 2674-2680.
9. M. H. Lee, J. H. Han, J. H. Lee, N. Park, R. Kumar, C. Kang and J. S. Kim, *Angew. Chem., Int. Ed.*, 2013, **52**, 6206–6209.
10. A. M. Dennis, W. J. Rhee, D. Sotto, S. N. Dublin and G. Bao, *ACS. Nano.*, 2012, **6**, 2917–2924.
11. B. Valeur, Ed.; Molecular Fluorescence. Principles and Applications Wiley-VCH: Weinheim, Germany, 2002.
12. J. Han and K. Burgess, *Chem. Rev.*, 2010, **110**, 2709–2728
13. T. J. Rink, R. Y. Tsien and T. J. Pozzan, *Cell. Biol.*, 1982, **95,** 189.
14. I. Kurtz and Bala R. S. ban, *Biophys. J.*, 1985, **48**, 499.
15. C. Balut, M. vande Ven, S. Despa, I. Lambrichts, M. Ameloot, P. Steels and I. Smets, *Kidney. Int.*, 2008, **73,** 226.
16. H. S. Peng, J. A. Stolwijk, L. N. Sun, J. Wegener and O. S. Wolfbeis, *Angew. Chem., Int. Ed.*, 2010, **49**, 4246–4249.
17. U. C. Saha, K. Dhara, B. Chattopadhyay, S. K. Mandal, S. Mondal, S. Sen, M. Mukherjee, S. V. Smaalen and P. Chattopadhyay, *Org. Lett.*, 2011, **13**, 4510–4513.
18. W. Shi, X. H. Li and H. M. Ma, *Angew. Chem. Int. Ed*., 2012, **51**, 6432–6435.
19. C. Balut, M. vandeven, S. Despa, I. Lambrichts, M. Ameloot, P. Steels and I. Smets, *Kidney. Int.*, 2008, **73**, 226.
20. C. S. Chen, *BMC. Cell. Biol.*, 2002, **3**, 21.
21. K. L. Tsai, S. M. Wang, C. C. Chen, T. H. Fong and M. L. Wu, *J. Physiol.*, 1997, **502**, 161–174.
22. M. Tantama, Y. P. Hung and G. Yellen, *J. Am. Chem. Soc.*, 2011, **133**, 10034–10037.

